

Simulation of transformation optics designed metamaterial for electromagnetic cloaking

Koppány Körmöczi / Zsolt Szabó

Received 2012-03-21, revised 2012-07-12, accepted 2012-07-31

Abstract

In this paper the numerical simulation of a metamaterial designed with transformation optics for hiding scattering objects is presented. The simulation environment is Matlab with the Partial Differential Equation Toolbox. The anisotropic and inhomogeneous electric permittivity and magnetic permeability of the metamaterial cloak are presented and transformed to fit the input requirements of the applied finite element solver. We show that the electromagnetic cloak is working not only under electromagnetic plane wave illumination, but it can hide objects exposed to point and line sources as well.

Keywords

electromagnetic cloaking · metamaterial · transformation optics · finite element method

Acknowledgement

This work has been supported by the János Bolyai Research Fellowship of the Hungarian Academy of Sciences.

Koppány Körmöczi

Department of Broadband Infocommunications and Electromagnetic Theory, BME, H-1111 Budapest, Goldmann Gy. tér 3, Hungary

Zsolt Szabó

Department of Broadband Infocommunications and Electromagnetic Theory, BME, H-1111 Budapest, Goldmann Gy. tér 3, Hungary
e-mail: szabo@evt.bme.hu

1 Introduction

The interaction of electromagnetic waves with matter is governed not only by its chemical composition, but micro or nanostructuring of materials can produce novel properties, which are not available in bulk form. In the research field of plasmonics [1], metamaterials [2, 3] and photonics crystals [4], nanostructures often with similar geometry are used to engineer new devices, which can extend the limits of lithography [5] and sub-wavelength imaging [6], cloak scattering objects [7], enhance the performance of sensors [8] and extend the bandwidth of interchip communication [9].

Artificial structures with the goal to fulfill a required electromagnetic behavior have been engineered for several decades. For example, antireflection coatings can produce a smooth transition of the refractive index at the interface of two dielectric media in order to minimize the reflection of electromagnetic waves. Electromagnetic screening can be produced with metallic structures (e.g. wires) to create a space free of electromagnetic radiations. In these examples the required behavior is obtained with the control of the electric permittivity. The research of metamaterials has started with the goal of producing materials with negative refractive index that is simultaneous negative electric permittivity and magnetic permeability for optical imaging without diffraction limit. Nowadays the metamaterial research extends in the direction to engineer arbitrary electromagnetic material properties. The possibility to manipulate not just the electric permittivity, however the magnetic permeability of artificial materials leads to novel applications and devices.

Recently electromagnetic cloaking of highly scattering objects has been successfully demonstrated, by designing the material parameters of a surrounding envelope with the method of transformation optics [7]. Cloaking means not just the elimination of the reflected component of the electromagnetic waves, which could be realized with a perfectly matched absorbing media. However, it is necessary to guide the flow of electromagnetic waves around the scattering objects to produce the illusion for arbitrarily positioned sources of electromagnetic radiation and observers that there is no scattering object. The full anisotropic electric permittivity and magnetic permeability ten-

sors are required to control the electric and the magnetic components of the electromagnetic radiations in order to hide the scattering objects.

The transformation optics is a new approach to the design of electromagnetic structures, by which the paths of electromagnetic waves are controlled by introducing a prescribed spatial variation in the effective material parameters [10, 11]. The material parameters required to guide the electromagnetic waves at the will of designers are determined with a conformal mapping [7]. The method of transformation optics is similar to the transformation, which describes how gravity warps the space-time in Einstein's Theory of General Relativity. The way to control electromagnetic waves is through a coordinate transformation between the real-space and a virtual-space, in which the wave trajectories are prescribed by the metrics of this non-real space.

Cloaking of scattering object has been shown at microwave [7, 13, 14], terahertz [15] and even at optical frequencies [16, 17]. The method of transformation optics has been successfully applied to design plasmonic devices as well [12]. Although the exact effective material parameters can be calculated with a suitable transformation [7], they often cannot be implemented because of the possible singularities in the spatial distribution of material parameters and limitations of fabrication technologies. The challenge of the engineer is to find a suitable transformation, which leads to implementable material parameters.

The anisotropic and inhomogeneous material parameters of the cloak can be constructed with layers of split ring resonators. The experiments show, that this configuration can hide the scattering cylinder for a monochromatic plane wave illumination [7]. At optical frequencies it is difficult to cloak a scattering object located in air for a non-monochromatic illumination, but working optical cloaks has been demonstrated for scatterers buried in a high dielectric media [16].

In this paper the material parameters of the electromagnetic cloak are presented under the condition of plane wave exposition and transformed to fit the requirements of the Matlab Partial Differential Equation Toolbox. It is demonstrated that the cloak is working properly under illumination with finite length sources as well.

2 Model description and the material parameters

To simulate the electromagnetic cloaking the Matlab Partial Differential Equation Toolbox, a general frequency domain finite element solver is employed to solve the anisotropic, inhomogeneous wave equation

$$\nabla \times (\mu_r^{-1} \nabla \times E) - \omega^2 \mu_0 \epsilon_r \epsilon_0 E = 0 \quad (1)$$

derived from the Maxwell equations, where E is the intensity of the electric field, ω is the angular frequency, ϵ_0 and μ_0 are the permittivity and permeability of the free space, while ϵ_r and μ_r are the complex inhomogeneous relative permittivity and permeability tensors. Note that this paper employs the $e^{i\omega t}$ notation.

The concealed scattering object is a copper cylinder standing in air with infinite length along the z axis of the real-space. Therefore the problem is invariant in the z direction, with the condition $\partial/\partial z = 0$. When the illumination shares the same symmetry, the Maxwell equations split in two unconnected subsets of partial differential equations, called TE and TM modes, which have analogue solution. The components of the TE mode in the rectangular coordinate system of the paper are E_z, H_x, H_y . As the problem is solved in frequency domain, the electric and the magnetic field components are complex functions. The computational space reduces to a two-dimensional domain, which can be solved in polar or Cartesian coordinate system with the wave equation in E_z

$$\nabla \times (\mu_r^{-1} \nabla \times E_z) - \omega^2 \mu_0 \epsilon_r \epsilon_0 = 0, \quad (2)$$

where E_z is the electric field in the direction of z .

The geometry of the cylinder, the frequency and the polarization of the illuminating electromagnetic wave are similar to those of [7], where the cloaking under plane wave illumination is demonstrated. In this paper line sources and superposition of line sources are considered as excitation. The line sources are placed parallel to the axis of the cylindrical scattering object as it is presented in Fig. 1. Therefore two-dimensional models are sufficient to simulate the evolution of the electromagnetic field in the computational space. In the two-dimensional computational space the line source reduces to a point, which generates cylindrical waves and the plane source reduces to a line, which creates a superposition of cylindrical waves.

To obtain the parameters of the cloak, the metamaterial surrounding the copper cylinder is designed with transformation optics [7, 18]. The coordinate transformation between the real-space real and the virtual-space is

$$r' = \frac{b-a}{a}r + a, \quad \theta' = \theta \quad (3)$$

with the constraints $0 < r < b, a < r' < b$, where r is the radial polar coordinate in the real-space, r' is the radial polar coordinate in the virtual-space, a is the inner radius and b is the outer radius of the cloak.

Solving the Maxwell equations with the coordinates of the warped space the parameters of the metamaterial can be calculated. The resulting cylindrical coordinate-based tensors [7] are

$$\epsilon_r = \mu_r \begin{bmatrix} \frac{r-a}{r} & 0 & 0 \\ 0 & \frac{r}{r-a} & 0 \\ 0 & 0 & \left(\frac{b}{b-a}\right)^2 \frac{r-a}{r} \end{bmatrix}. \quad (4)$$

For TE mode the electric permittivity reduces to a scalar

$$\epsilon_r = \left(\frac{b}{b-a}\right)^2 \frac{r-a}{r}, \quad (5)$$

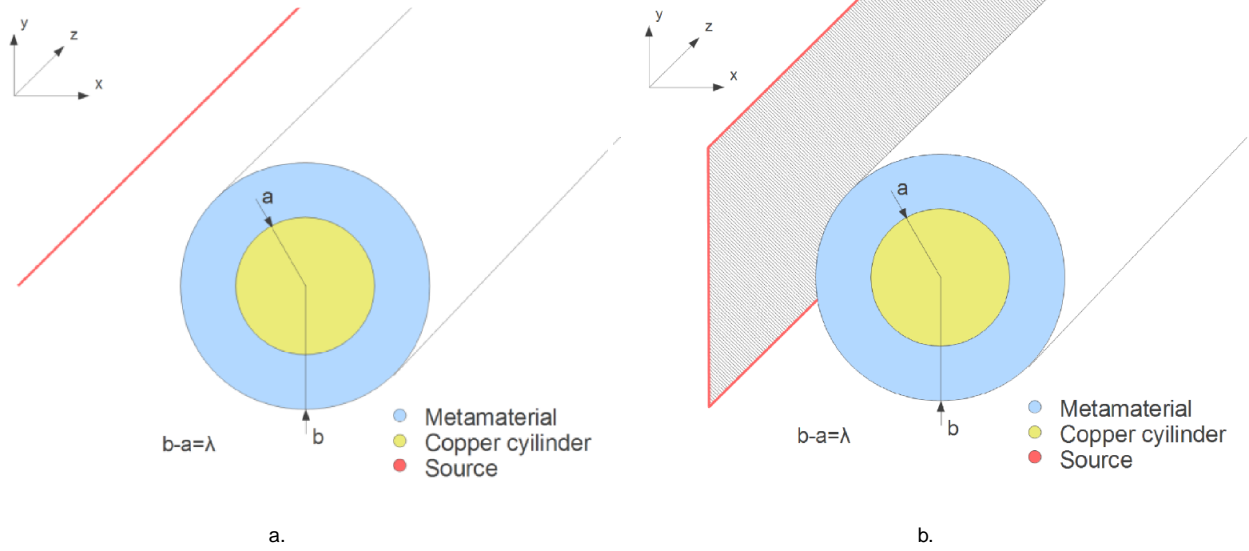


Fig. 1. The geometry of the investigated arrangement with the copper cylinder and the surrounding electromagnetic cloak is shown. In (a) the excitation

is the line source, while in (b) the configuration is illuminated with electromagnetic wave generated by the plane source with finite configuration extent.

and the magnetic permeability has the form

$$\mu_r = \begin{bmatrix} \frac{r-a}{r} & 0 \\ 0 & \frac{r}{r-a} \end{bmatrix}. \quad (6)$$

The numerical solver of Matlab calculates partial derivatives along the Cartesian bases. Therefore the tensor of the magnetic permeability is transformed to Cartesian coordinates

$$\begin{bmatrix} \mu_{xx} & \mu_{xy} \\ \mu_{yx} & \mu_{yy} \end{bmatrix} = R^{-1}(-\theta) \begin{bmatrix} \mu_{rr} & \mu_{r\theta} \\ \mu_{\theta r} & \mu_{\theta\theta} \end{bmatrix} R(-\theta), \quad (7)$$

where R is the rotation matrix around the z axis

$$R(\alpha) = \begin{bmatrix} \cos \alpha & -\sin \alpha \\ \sin \alpha & \cos \alpha \end{bmatrix}. \quad (8)$$

The coordinate transformation is illustrated in Fig. 2, where the position vector \mathbf{r} is plotted with red, the blue represents the magnetic field intensity vector, the orange denotes the components of the magnetic field in polar coordinates, while the Cartesian components of the magnetic field are shown in green.

The magnetic field intensity in Cartesian coordinates can be obtained with the rotation of the polar base by θ in clockwise direction. The inverse of the rotation matrix is equal with its transpose, and $R(-\theta) = R^T(\theta)$, therefore

$$\begin{bmatrix} \mu_{xx} & \mu_{xy} \\ \mu_{yx} & \mu_{yy} \end{bmatrix} = \begin{bmatrix} \cos \theta & -\sin \theta \\ \sin \theta & \cos \theta \end{bmatrix} \begin{bmatrix} \frac{r-a}{r} & 0 \\ 0 & \frac{r}{r-a} \end{bmatrix} \begin{bmatrix} \cos \theta & \sin \theta \\ -\sin \theta & \cos \theta \end{bmatrix}. \quad (9)$$

After the matrix multiplications, the Cartesian components of the magnetic permeability tensor in a point of the cloak with

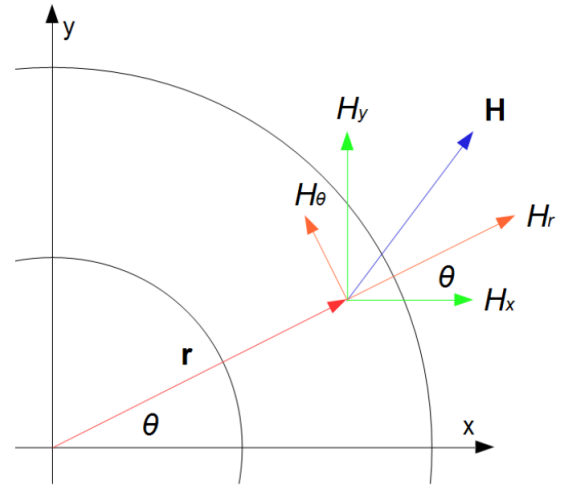


Fig. 2. Transformation of the magnetic field intensity from polar to Cartesian coordinates with θ rotation in clockwise direction.

coordinates (x, y) are

$$\begin{aligned} \mu_{xx} &= \frac{r-a}{r} \cos^2 \theta + \frac{r}{r-a} \sin^2 \theta, \\ \mu_{xy} &= \frac{r-a}{r} \cos \theta \sin \theta - \frac{r}{r-a} \sin \theta \cos \theta, \\ \mu_{yx} &= \frac{r-a}{r} \cos \theta \sin \theta - \frac{r}{r-a} \sin \theta \cos \theta, \\ \mu_{yy} &= \frac{r-a}{r} \sin^2 \theta + \frac{r}{r-a} \cos^2 \theta, \end{aligned} \quad (10)$$

where the distance $r = \sqrt{x^2 + y^2}$ and the angle $\theta = \arctan(y/x)$. The computational cost of the trigonometric functions can be avoided with the following relations

$$\begin{aligned} \sin \left[\arctan \left(\frac{y}{x} \right) \right] &= \frac{\frac{y}{x}}{\sqrt{1 + \left(\frac{y}{x} \right)^2}}, \\ \cos \left[\arctan \left(\frac{y}{x} \right) \right] &= \frac{1}{\sqrt{1 + \left(\frac{y}{x} \right)^2}}. \end{aligned} \quad (11)$$

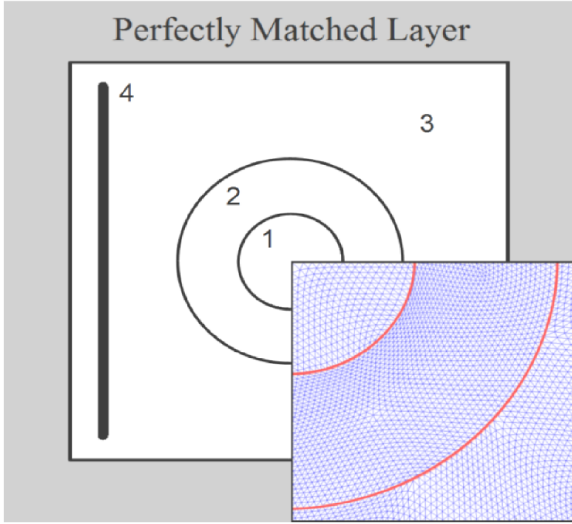


Fig. 3. The computational domain and the triangular mesh. The scattering object (copper cylinder) is denoted with 1, the metamaterial cloak is 2, the surrounding air region is 3, while 4 is the line source, which is implemented with inhomogeneous Dirichlet boundary condition.

In order to fabricate the metamaterial cloak, further simplifications of the material parameters (5) and (6) are required. The exact material parameters can be approximated with a reduced set of material parameters [7], which has the same dispersion properties as (5) and (6) in the form of

$$\varepsilon_r = \left(\frac{b}{b-a} \right)^2, \mu_r = \begin{bmatrix} \left(\frac{r-a}{r} \right)^2 & 0 \\ 0 & 1 \end{bmatrix}. \quad (12)$$

These expressions can be transformed to a similar form as (10).

3 Implementation of the boundary value problem

In the general anisotropic, inhomogeneous wave equation (1) the inverse of the relative magnetic permeability tensor appears, which in Cartesian coordinates takes the form

$$\begin{aligned} \mu_{xx}^{-1} &= \frac{r-a}{r} \sin^2 \theta + \frac{r}{r-a} \cos^2 \theta, \\ \mu_{xy}^{-1} &= -\frac{r-a}{r} \sin \theta \cos \theta + \frac{r}{r-a} \sin \theta \cos \theta, \\ \mu_{yx}^{-1} &= -\frac{r-a}{r} \sin \theta \cos \theta + \frac{r}{r-a} \sin \theta \cos \theta, \\ \mu_{yy}^{-1} &= \frac{r-a}{r} \cos^2 \theta + \frac{r}{r-a} \sin^2 \theta \end{aligned} \quad (13)$$

and substituting the material parameters in (1), results in the following explicit form

$$\begin{aligned} \frac{\partial}{\partial x} \left(\mu_{yx}^{-1} \frac{\partial E_z}{\partial y} - \mu_{yy}^{-1} \frac{\partial E_z}{\partial x} \right) - \\ \frac{\partial}{\partial y} \left(\mu_{xx}^{-1} \frac{\partial E_z}{\partial y} - \mu_{xy}^{-1} \frac{\partial E_z}{\partial x} \right) - \omega^2 \mu_0 \varepsilon_r \varepsilon_0 E_z = 0. \end{aligned} \quad (14)$$

The template of the Matlab PDE Toolbox equation is

$$-\nabla \cdot (c \nabla u) + au =$$

$$-\frac{\partial}{\partial x} \left(c_1 \frac{\partial u}{\partial x} + c_2 \frac{\partial u}{\partial y} \right) - \frac{\partial}{\partial y} \left(c_3 \frac{\partial u}{\partial x} + c_4 \frac{\partial u}{\partial y} \right) + au = f, \quad (15)$$

where u is a complex scalar function, a and f are scalar parameters and c is the matrix parameter of the equation.

Comparing (14) and (15) the correspondences are

$$\begin{aligned} c &= \begin{bmatrix} c_1 & c_2 \\ c_3 & c_4 \end{bmatrix} = \begin{bmatrix} \mu_{yy}^{-1} & -\mu_{yx}^{-1} \\ -\mu_{xy}^{-1} & \mu_{xx}^{-1} \end{bmatrix}, \\ a &= -\omega^2 \mu_0 \varepsilon_0 \left(\frac{b}{b-a} \right)^2 \frac{r-a}{r}, \\ f &= 0 \end{aligned} \quad (16)$$

and the scalar function u corresponds to the E_z component of the electromagnetic field.

To simulate the electromagnetic wave propagation the open-bounded space has to be truncated to a finite region. The computational domain is enclosed by reflectionless absorbing boundary. In this paper the Perfectly Matched Layer (PML) and the Sommerfeld Absorbing Boundary Condition (ABC) are used.

The PML is a wavelength thick artificial absorbing layer around the examined region, which can be implemented in the Matlab Partial Differential Equation Toolbox with the operator

$$\nabla' = \sum_{k=1}^2 \hat{x}_k \frac{1}{1 + i \frac{\sigma(x_k)}{\omega}} \frac{\partial}{\partial x_k}, \quad (17)$$

and the absorbing function is

$$\sigma(x_k) = \frac{c}{\tilde{x}_k - x_k}, \quad (18)$$

where \hat{x}_k are the unit vectors of the Cartesian coordinate system, \tilde{x}_k are the components of the position vector at the border of the PML in the \hat{x}_k direction, c is the speed of light in vacuum, ω is the angular frequency and $i = \sqrt{-1}$ is the imaginary unit.

In case of the Sommerfeld ABC the computational domain can have circular form. The expression of this boundary condition for TE waves is

$$\lim_{r \rightarrow \infty} \sqrt{r} \left(\frac{\partial E_z}{\partial r} + ik E_z \right) = 0. \quad (19)$$

In two-dimensions this relation can be expressed as

$$\frac{\partial E_z}{\partial n} + ik E_z + \frac{E_z}{2R} = 0, \quad (20)$$

which is a modified Neumann boundary condition, where n is the outward normal vector of the border, k is the wavenumber of the outgoing electromagnetic radiation and R is the radius of the circular computational domain.

The PML is highly performing boundary condition; however the Sommerfeld condition fits to the circular symmetry of the current problem. The equations implementing the PML and the

Fig. 4. In (a) the electromagnetic wave generated by the finite length line source is shown, while (b) presents the scattering from the bare copper cylinder. The simulations of (c) and (d) demonstrate the electromagnetic cloaking with the exact and the reduced set of material parameters.

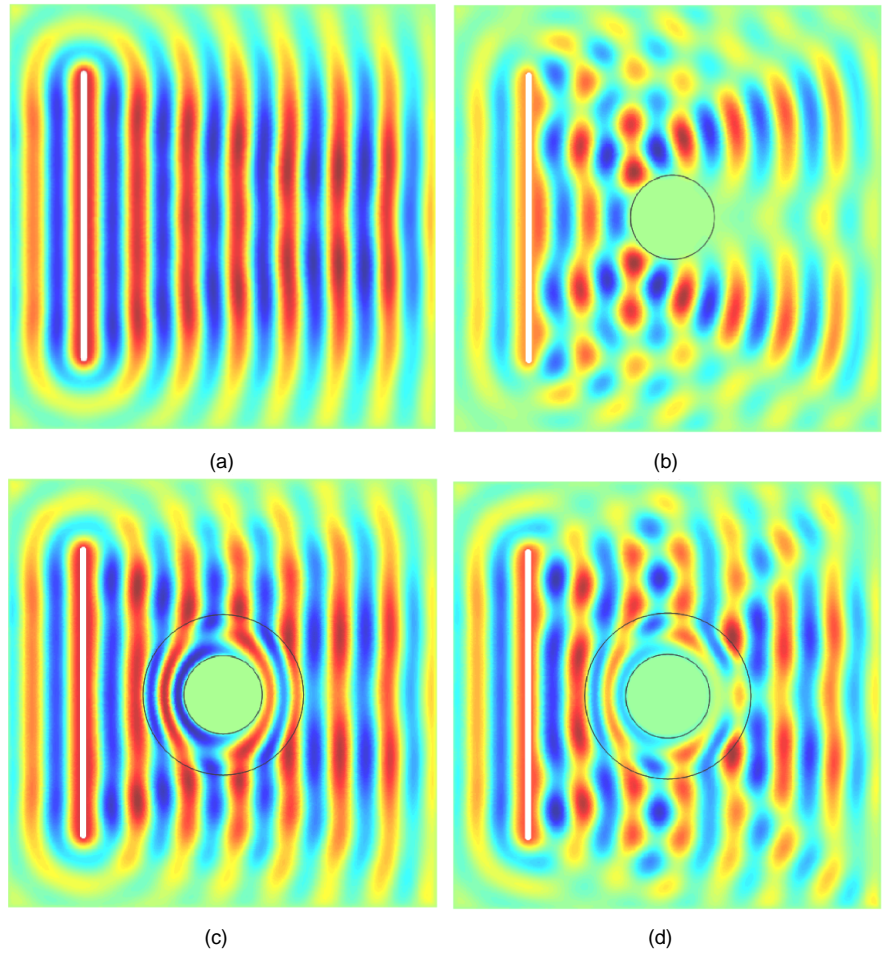
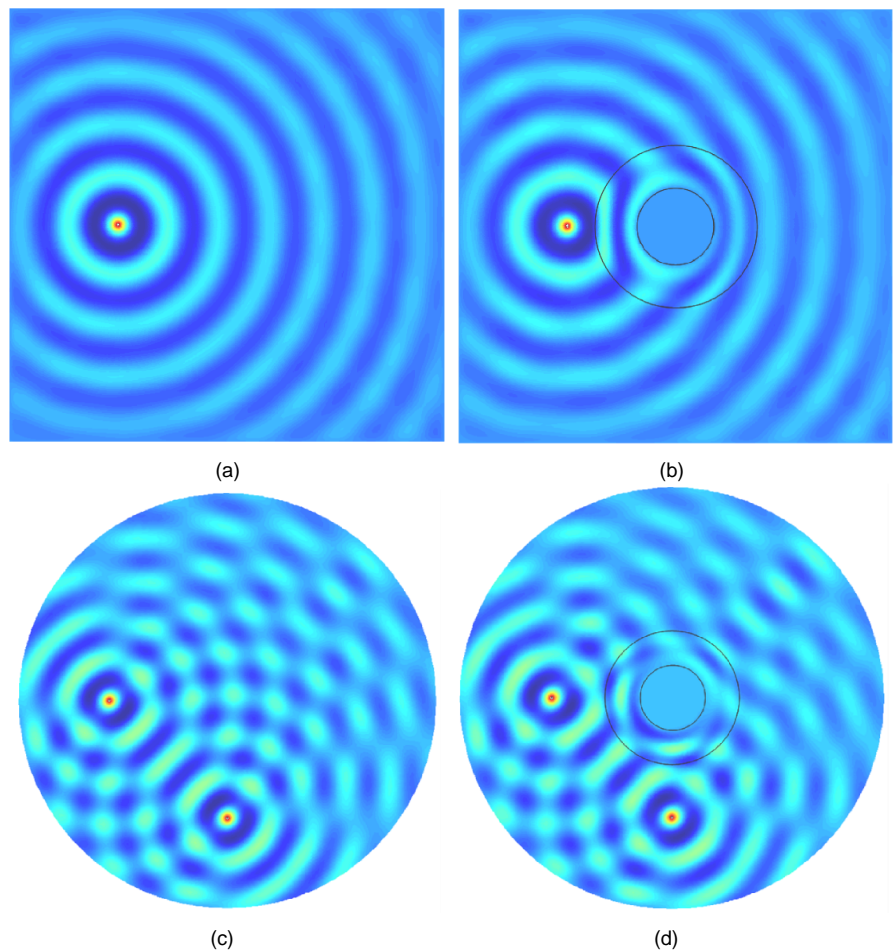


Fig. 5. In (a) the wave pattern is illustrated in case of a single point source, while (b) shows the concealment. For two interfering point sources the electric field distribution is plotted in (c), while (d) shows the electromagnetic invisibility effect.



Tab. 1. This table presents the equations, which implement the PML and the Sommerfeld ABC to truncate the computational domain. In the first row the Matlab expressions of the partial differential equation and the Neumann condition can be seen, while the second row presents the coefficients.

PML	Sommerfeld
$-\nabla \cdot (c\nabla u) + au = f$	$cn\nabla u + qu = g$
$c = \text{diag}\left(\frac{1}{1+i\sigma(x)}, \frac{1}{1+i\sigma(y)}\right)$	$c = 1, q = ik + \frac{1}{2R}, g = 0$

Sommerfeld ABC in the Matlab Partial Differential Equation Toolbox are summarized in Table 1.

The sources of the electromagnetic radiation can be introduced in the computational domain with inhomogeneous Dirichlet boundary condition for the line and also for the point sources. The magnitude of the incident electric field is considered equal to one. The computational domain includes the scattering object, the cloak, the line source and the PML region as shown in Fig. 3. The inset presents the triangular mesh of the calculations in a region of the scattering object and the cloak. This mesh is obtained after four steps of refinements.

The Matlab code, which implements the presented procedure can be downloaded from [19]. After the mesh generation and refinement, the software calculates and plots the real part of the electric field intensity E_z . To investigate the steady-state behavior of the cloak, the frequency domain solution E_z is multiplied by a time dependent factor $e^{i2\pi n/n_f}$, where n is an integer from 0 to n_f , to obtain the time dependent behavior and to produce animations with n_f frames for one period of the electromagnetic wave propagation.

The performance of the cloak can be measured with the mean square error

$$\epsilon = \frac{1}{N} \sqrt{\sum_{i=1}^n \left(\frac{E_i - E_i^S}{E_i^S} \right)^2} \quad (21)$$

of the difference between the electric field magnitude E_i and the magnitude of the electric field produced by standalone sources E_i^S in a point outside of the cloak. It is ensured that the mesh is not changed when the scattering object and the cloak are excluded from the calculations. Then the mean square error can be easily generated comparing the electric fields with the same mesh node number.

4 Illumination of the electromagnetic cloak

The simulations presenting the electromagnetic cloaking of the copper cylinder are shown in Fig. 4 and Fig. 5. In Fig. 4.a the field produced by the standalone line source is plotted. The scattering of the electromagnetic wave from the standalone copper cylinder (without the cloak) is presented in Fig. 4.b. The simulation of Fig. 4.c shows the distribution of the electric field when the copper cylinder is surrounded by the cloak with the exact material parameters (5) and (6). For this case a small mean square error is obtained, which shows that the concealment can successfully hide the copper cylinder under line source illumina-

tion. For the reduced set of material parameters (12) the distribution of the electric field intensity is plotted in Fig. 4.d. In this case the cloaking is not perfect; nevertheless it is in agreement with the results of [7], where the cloaking with plane wave illumination is studied. For the point source generating cylindrical waves, the electric field distribution is presented in Fig. 5.a. In Fig. 5.b the concealment under point source illumination is demonstrated for the exact material parameters, while Fig 5.c and Fig 5.d shows the field distribution of two interfering point sources without and with the cloak. Comparing the simulations presented in Fig. 5.a and Fig. 5.b or Fig. 5.c and Fig. 5.d, it can be observed that the cloak works properly in the near field of the sources as well.

5 Conclusion

We have presented a method, and derived the required mathematical expressions to simulate the electromagnetic cloaking with the Matlab Partial Differential Equation Toolbox. Our software implementing the presented procedure is freely available online [19]. The algorithm and the animations presenting the wave propagation around the cloaked object can be useful in advanced electromagnetic courses.

The results of the simulations show that the cloak with the considered material parameters works properly not only under plane wave illumination, but the invisibility is guaranteed for all kinds of electromagnetic sources producing TE waves polarized along the axis. Extrapolating the simulation results it can be confirmed that the cloak can work properly in the near field of antennas as well. In case of an object with finite volume the elements of the material parameter tensors are more complicated and a full three-dimensional simulation is required.

References

- 1 **Maier SA**, *Plasmonics: Fundamentals and Applications*, Springer, 2010, ISBN 9780387331508.
- 2 **Solymar L, Shamonina E**, *Waves in Metamaterials*, Oxford University Press, 2009, ISBN 9780199215331.
- 3 **Munk BA**, *Metamaterials: A Critique and Alternatives*, Wiley, 2009, ISBN 9780470423868.
- 4 **Joannopoulos JD, Johnson SG, Winn JN, Meade RD**, *Photonic Crystals: Molding the Flow of Light*, Princeton University Press, 2008, ISBN 9780691124568.
- 5 **Pan L, Park Y, Xiong Y, Ulin-Avila E, Wang Y, Zeng L, Xiong S, Rho J, Sun C, Bogy DB, Zhang X**, *Maskless Plasmonic Lithography at 22 nm Resolution*, Nature Scientific Reports, **1**(175), (2011), DOI 10.1038/srep00175.
- 6 **Rho J, Ye Z, Xiong Y, Yin X, Liu Z, Choi H, Bartal G, Zhang X**, *Spherical Hyperlens for Two-Dimensional Sub-Diffractive Imaging at Visible Frequencies*, Nature Communications, **1**(143), (2010), DOI 10.1038/ncomms1148.
- 7 **Schurig D, Mock JJ, Justice BJ, Cummer SA, Pendry JB, Starr AF, Smith DR**, *Metamaterial Electromagnetic Cloak at Microwave Frequencies*, Science, **314**, (2006), 977–980, DOI 10.1126/science.1133628.
- 8 **Lukyanchuk B, Zheludev NI, Maier SA, Halas NJ, Nordlander P, Giessen H, Chong CT**, *The Fano Resonance in Plasmonic Nanostructures and Metamaterials*, Nature Materials, **9**, (2010), 707–715, DOI 10.1038/nmat2810.

- 9 **Schuller J, Barnard E, Cai W, Jun YC, White J, Brongersma ML.** *Plasmonics for Extreme Light Concentration and Manipulation*, *Nature Materials*, **9**(3), (2010), 193–204, DOI 10.1038/nmat2630.
- 10 **Pendry JB, Schurig D, Smith DR.** *Controlling Electromagnetic Fields*, *Science*, **312**, (2006), 1780–1782, DOI 10.1126/science.1125907.
- 11 **Leonhardt U.** *Optical Conformal Mapping*, *Science*, **312**, (2006), 1777–1780, DOI 10.1126/science.1126493.
- 12 **Zentgraf T, Liu Y, Mikkelsen MH, Valentine J, Zhang X.** *Plasmonic Luneburg and Eaton Lenses*, *Nature Nanotechnology*, **6**, (2011), 151–155, DOI 10.1038/nnano.210.282.
- 13 **Hofer WJR, Gi-Ho P, Li E-P.** *Time Domain Study of Electromagnetic Cloaks for Wideband Invisibility under Transient Illumination*, *Microwave Symposium Digest (MTT)*, 2010 IEEE MTT-S International, (2010), 89–92, DOI 10.1109/mwsym.2010.5515284.
- 14 **Alitalo P, Tretyakov SA.** *Broadband Electromagnetic Cloaking Realized with Transmission-Line and Waveguiding Structures*, *Proceedings of the IEEE*, **99**(10), (2011), 1646–1659, DOI 10.1109/jproc.2010.2093471.
- 15 **Zhou F, Bao Y, Cao W, Stuart CT, Gu J, Zhang W, Sun C.** *Hiding a Realistic Object Using a Broadband Terahertz Invisibility Cloak*, *Nature Scientific Reports*, **1**, (2011), 78, DOI 10.1038/srep00078.
- 16 **Valentine J, Li J, Zentgraf T, Bartal G, Zhang X.** *An Optical Cloak Made of Dielectrics*, *Nature Materials*, **8**, (2009), 568–571, DOI 10.1038/nmat2461.
- 17 **Huang Y, Feng Y, Jiang T.** *Electromagnetic Cloaking by Layered Structure of Homogeneous Isotropic Materials*, *Optics Express*, **15**, (2007), 11133–11141, DOI 10.1364/oe.15.011133.
- 18 **Kildishev AV, Cai W, Chettiar UK, Shalaev VM.** *Transformation optics: Approaching Broadband Electromagnetic Cloaking*, *New Journal of Physics*, **10**, (2008), 115029, DOI 10.1088/1367-2630/10/11/115029.
- 19 **Körmöczi K, Szabó Z.** *Cloaking Source code*, <http://www.mathworks.com/matlabcentral/fileexchange/35706>, <http://www.sourceforge.net/projects/cloaking/>.